Neutron diffraction and heat capacity studies of $PrCoO_3$ and $NdCoO_3$

Karel Knížek,[1] Jiří Hejtmánek,[1] Zdeněk Jirák,[1] Petr Tomeš,[2] Paul Henry,[3] and Gilles André[4]
[1]*Institute of Physics ASCR, Cukrovarnická 10, 162 00 Prague 6, Czech Republic*
[2]*Solid State Chemistry and Catalysis, Empa, Ueberlandstr. 129, CH-8600 Duebendorf, Switzerland*
[3]*Institut Laue Langevin, 6 rue Jules Horowitz, 38042 Grenoble Cedex 9, France*
[4]*Laboratoire Léon Brillouin, CEA-CNRS, CEA-Saclay, 91191 Gif-s-Yvette Cedex, France*
(Received 26 January 2009; revised manuscript received 6 March 2009; published 3 April 2009)

The crystal structures of perovskites $NdCoO_3$ and $PrCoO_3$ have been studied by neutron powder diffraction over a temperature range from 100 to 1000 K. An anomalous isotropic expansion of CoO_6 octahedra is observed at two successive temperatures corresponding to the spin transitions of Co^{3+} from low spin (LS) ($S=0$) to high spin (HS) ($S=2$) and intermediate spin (IS) ($S=1$). At the second spin transition, a significant change in the octahedral tilt is encountered, as well. The heat capacity measurements show broad excess peaks at both transitions and the integral entropy change for each of them is estimated to be ≈ 10 J K^{-1} mol^{-1}. The structural and specific heat anomalies are interpreted within the LS-LS/HS-IS model of the Co^{3+} spin transitions.

DOI: 10.1103/PhysRevB.79.134103 PACS number(s): 61.05.fm, 75.30.Wx, 65.40.Ba

I. INTRODUCTION

Interest in the perovskite cobaltites $LnCoO_3$ is associated with magnetic and electronic transitions which are related to changes in the local Co^{3+} spin states and to the character of itinerant carriers. All the $LnCoO_3$ (Ln=La, Y, and rare-earth metal) systems show an insulating ground state based on the diamagnetic low-spin state of trivalent cobalt that in the limit of fully localized electrons in strong crystal field corresponds to filled t_{2g} levels and empty e_g states (LS, $t_{2g}^6 e_g^0$, and $S=0$). With increasing temperature they undergo two magnetic transitions connected with excitations either to the intermediate spin (IS, $t_{2g}^5 e_g^1$, and $S=1$) or to the high spin state (HS, $t_{2g}^4 e_g^2$, and $S=2$). The second magnetic transition is accompanied by an insulator-metal (I-M) transition.

The spin transitions are further manifested by observable changes in the crystal structure since the ionic radius of Co^{3+} increases with increasing spin state and produces anomalies in thermal expansion.[1–7] Additionally, Co^{3+} ion in IS or HS state is expected to be Jahn-Teller active and some kind of CoO_6 octahedra distortion can be anticipated.

The data on the lattice thermal expansion, obtained for $LnCoO_3$ by x-ray powder diffraction (see, e.g., Ref. 5), show that the transition temperatures increase with decreasing Ln radius. In particular, the characteristic temperatures of the transitions are ≈ 70 and 540 K for $LaCoO_3$, ≈ 260 and 600 K for $PrCoO_3$, and ≈ 340 and 630 K for $NdCoO_3$, and two distinct maxima in the dilatation coefficient are detected.

The advantage of powder neutron diffraction is a higher sensitivity to oxygen positions, which allows a reliable determination of the Co-O bond thermal expansion. Very systematic study has been performed for $LaCoO_3$.[3] Other systems already studied by neutron diffraction are $YCoO_3$ (Refs. 8 and 9) and $NdCoO_3$,[10,11] whereas the lattice expansion data and structure determination at selected temperatures only have been reported for $PrCoO_3$.[12,13]

The present neutron diffraction study has been performed with the aim to compare the structural anomalies associated with Co^{3+} spin transitions in orthorhombic systems $LnCoO_3$ with those in the rhombohedral $LaCoO_3$. The phases $PrCoO_3$ and $NdCoO_3$ were chosen since their spin transitions are well separated in temperature in contrast to $LnCoO_3$ with smaller Ln. The structural results include a detailed determination of the temperature evolution of Co-O bonds and Co-O-Co angles in CoO_6 octahedra and are complemented with the heat capacity measurements.

II. EXPERIMENTAL

Samples $NdCoO_3$ and $PrCoO_3$ were prepared by a solid-state reaction from stoichiometric amounts of Co_2O_3 and respective oxides Nd_2O_3 and Pr_6O_{11}. The precursor powders were mixed, pressed in the form of pellets, and sintered at 1200 °C for 100 h under air.

The structural data have been obtained by neutron diffraction experiments, performed at low temperature in LLB (Saclay, France) on the G41 diffractometer using a wavelength of 2.422 Å and at high temperature in ILL (Grenoble, France) on the D20 diffractometer using a wavelength of 1.361 Å. Typical neutron diffraction patterns of $PrCoO_3$ and $NdCoO_3$ at room temperature are displayed in Fig. 1. The high-temperature measurements were performed in a furnace with a quartz tube flowed by air. The obtained neutron diffraction data were analyzed by a Rietveld method with the help of the FULLPROF program (version 3.30-Jun2005-LLB JRC).

The specific heat below room temperature was measured by PPMS device (Quantum Design) using the two-τ model of the relaxation method and at high temperature was determined by DSC using a NETZSCH DSC 404 C Pegasus in a synthetic air atmosphere at a heating rate of 20 K min^{-1}.

III. RESULTS AND DISCUSSION

The neutron diffraction confirmed orthorhombic *Pbnm* symmetry for both $PrCoO_3$ and $NdCoO_3$ over the whole experimental temperature range. The occupancy of oxygen sites was found close to the stoichiometric value of 3 within

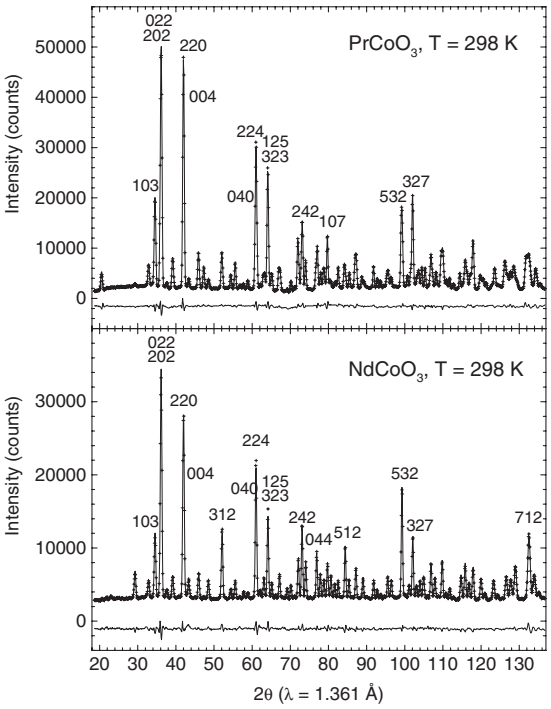

FIG. 1. Neutron diffraction of $PrCoO_3$ and $NdCoO_3$ at room temperature. The main reflections are indexed.

the standard deviation (± 0.01). The refined structural parameters at selected temperatures of 150, 300, 500, and 800 K are presented in Table I. At room temperature, the structural parameters agree with the values determined for $PrCoO_3$ in Refs. 12 and 13 and for $NdCoO_3$ in Ref. 10.

The temperature dependence of lattice parameters determined by neutron diffraction is displayed in Fig. 2. The data agree with the dependence determined previously by x-ray diffraction in Ref. 5. Also displayed in Fig. 2 is the orthorhombic distortion in $PrCoO_3$ and $NdCoO_3$ which is defined as a deviation of the *Pbnm* lattice parameters with respect to the pseudocubic ones $\sqrt{\Sigma(a_i-\bar{a})^2}/\bar{a}$, where $a_i=a$, b, and $c/\sqrt{2}$ and $\bar{a}$ is the average of a_i.

For perovskites with smaller *A* cations (rare-earth metal in our case) the relation between lattice parameters $b>c/\sqrt{2}>a$ is typical and is observed from $YCoO_3$ to $SmCoO_3$.[5,13] This is the so-called *O* type, where tilting of the octahedra network is the dominant source of the orthorhombic distortion. The tilting becomes smaller with increasing size of the rare-earth cation and so does the orthorhombic distortion.

The situation is different for $NdCoO_3$ and $PrCoO_3$, where a small local distortion of the CoO_6 octahedra, namely, deviation of the O-Co-O angle from 90° common for orthoperovskites (see, e.g., Ref. 14) starts to prevail over the octahedra tilting. As a consequence the relation of lattice parameters changes to $a>c/\sqrt{2}>b$ and although the tilting of CoO_6 octahedra is still decreasing with increasing Ln radius, the orthorhombic distortion develops in the opposite direction. Thus the octahedra tilting is smaller, i.e., Co-O-Co bond angle is more linear, for Pr perovskite with bigger Ln ionic radius ($r_{Pr^{3+}}=1.179$ Å) than for Nd ($r_{Nd^{3+}}=1.163$ Å), but the orthorhombic distortion is larger for $PrCoO_3$.

The same reasoning accounts for the temperature dependence of lattice parameters. At the lowest temperatures, the main effect comes from a higher thermal expansion of ionic Ln-O bonds compared to more covalent Co-O bonds. Consequently, the octahedral tilt is decreasing but the orthorhombic distortion of the $a>c/\sqrt{2}>b$ type is increasing. The change in the slope of the orthorhombic distortion above 230 K for $PrCoO_3$ and 300 K for $NdCoO_3$ reflects an anomalous increase in Co-O bond lengths due to the spin-state transition of Co^{3+} ions. In the case of $NdCoO_3$ the lattice parameters cross around $\approx$600 K and above this temperature the relation changes to $b>c/\sqrt{2}>a$, which is typical for $LnCoO_3$ with smaller Ln.

The refined Co-O bond lengths and Co-O-Co bond angles for $PrCoO_3$ are displayed in the Fig. 3. The CoO_6 octahedra are close to regular geometry at all temperatures. In particular, there is no significant sign of Jahn-Teller-type distortion. The temperature evolution of the two Co-O-Co bond angles in the *Pbnm* structure can be divided into three regions. From low temperature up to about 450 K the more straight Co-O_c-Co angle is almost constant while the Co-O_{ab}-Co angle is linearly increasing with temperature. Similar low-temperature behavior has been observed also in other orthoperovskites (see, e.g., the data for $NdFeO_3$ in Ref. 15). At $\sim$450 K the angles become equal and above this temperature these are apparently constant within the error bars. However, closer inspection reveals that the data do not scatter randomly around a constant value but exhibit certain trends; in particular, the angles are slightly decreasing within the temperature range of 450–800 K and slightly increasing in the third region above 800 K. This behavior may be more clearly recognized in the evolution of averaged Co-O-Co bond angles in Fig. 4.

The results displayed for $NdCoO_3$ in Fig. 3 are similar as to the temperature evolution, but they are less accurate due to stronger overlap of diffraction peaks compared to $PrCoO_3$. The overlap of peaks brings along instability of refinement and correlation of refined parameters. In particular, special care was given to a correlation between *x* and *y* coordination of oxygen O_{ab} with a consequent correlation between the two Co-O_{ab} bond lengths lying in the *ab* plane.

The low-temperature behavior of bond angles of $NdCoO_3$ up to about 500 K is similar as for $PrCoO_3$, i.e., the more straight Co-O_c-Co angle is almost constant while the Co-O_{ab}-Co angle is linearly increasing with temperature. Above this temperature the angles are slightly decreasing and above $\sim$850 K these are practically constant. Similarly as in the case of $PrCoO_3$, the scale of these trends is comparable with the error bars and the behavior may be more clearly recognized in the evolution of averaged Co-O-Co bond angles in Fig. 4.

The present values of Co-O bond lengths and Co-O-Co bond angles agree essentially with the values determined over the temperature range of 3–540 K in Ref. 10. As regard to the Co-O bond lengths and Co-O-Co bond angles determined over the temperature range of 300–1100 K in Ref. 11, there is an agreement in the evolution of average values; however, we have not observed the CoO_6 octahedra distortion reported by the authors.

The lower panels of Fig. 3 display the isotropic atomic displacement parameters *B* (Å^2), which are related to the atomic mean-square displacement $\langle u^2\rangle$ (Å^2) by the relation

TABLE I. Structural parameters of $PrCoO_3$ and $NdCoO_3$ at selected temperatures as refined from neutron powder diffraction data, with space group *Pbnm*. Calculated standard deviations are in parentheses.

	$PrCoO_3$				$NdCoO_3$			
T (K)	150	300	500	800	150	300	500	800
a (Å)	5.3638(12)	5.3737(3)	5.4003(5)	5.4423(6)	5.3371(19)	5.3438(6)	5.3705(6)	5.4126(7)
b (Å)	5.3300(12)	5.3395(3)	5.3700(5)	5.4193(6)	5.3293(17)	5.3345(5)	5.3638(6)	5.4167(7)
c (Å)	7.5608(23)	7.5729(5)	7.6129(7)	7.6752(8)	7.5403(27)	7.5478(9)	7.5865(9)	7.6490(10)
Refinable atom coordinates: Pr,Nd $4c(x,y,1/4)$, Co $4b(1/2,0,0)$, O $14c(x,y,1/4)$, O $28d(x,y,z)$								
Pr, Nd(x)	0.9975(9)	0.9957(6)	0.9962(7)	0.9946(10)	0.9920(8)	0.9924(8)	0.9936(7)	0.9930(10)
Pr, Nd(y)	0.0312(5)	0.0290(4)	0.0267(4)	0.0258(6)	0.0372(3)	0.0352(3)	0.0322(4)	0.0307(5)
O1(x)	0.0657(7)	0.0669(3)	0.0670(4)	0.0672(6)	0.0679(8)	0.0687(8)	0.0688(9)	0.0696(12)
O1(y)	0.4853(4)	0.4946(3)	0.4938(4)	0.4940(6)	0.4838(5)	0.4836(5)	0.4835(7)	0.4829(9)
O2(x)	−0.2914(3)	−0.2822(2)	−0.2813(2)	−0.2813(3)	−0.2931(6)	−0.2923(7)	−0.2920(5)	−0.2924(7)
O2(y)	0.2920(3)	0.2827(2)	0.2818(2)	0.2821(3)	0.2934(7)	0.2932(6)	0.2928(5)	0.2934(7)
O2(z)	0.0267(3)	0.0357(2)	0.0353(2)	0.0357(3)	0.0300(4)	0.0293(4)	0.0280(4)	0.0304(5)
Selected bond distances and angles								
Co-O average (Å)	1.926(2)	1.928(1)	1.938(1)	1.954(2)	1.925(3)	1.927(3)	1.936(2)	1.955(3)
Co-O-Co average (deg)	157.9(2)	158.3(1)	158.5(2)	158.4(2)	156.7(3)	156.8(3)	157.1(3)	156.5(4)
Co-O_c(Å) × 2	1.924(2)	1.927(1)	1.938(1)	1.954(1)	1.922(3)	1.924(3)	1.934(1)	1.951(1)
Co-O_{ab}(Å) × 2	1.927(2)	1.928(1)	1.937(1)	1.953(2)	1.927(4)	1.925(4)	1.934(3)	1.952(4)
Co-O_{ab}(Å) × 2	1.928(2)	1.929(1)	1.938(1)	1.957(2)	1.927(4)	1.931(3)	1.939(3)	1.960(4)
Co-O_c-Co(deg) × 1	158.4(3)	158.4(1)	158.4(2)	158.3(3)	157.6(3)	157.4(3)	157.4(4)	157.1(5)
Co-O_{ab}-Co(deg) × 2	157.6(2)	158.2(1)	158.5(1)	158.4(2)	156.2(3)	156.6(3)	157.0(3)	156.3(4)
Isotropic atomic displacement parameters B_{iso} (Å^2)								
Pr, Nd	0.52(7)	0.53(3)	0.83(3)	1.35(4)	0.30(5)	0.32(5)	0.55(2)	1.04(3)
Co	0.15(7)	0.21(4)	0.32(4)	0.41(5)	0.18(9)	0.22(9)	0.28(6)	0.48(8)
O1	0.50(7)	0.52(4)	0.77(3)	1.32(4)	0.35(7)	0.43(7)	0.57(4)	1.10(5)
O2	0.48(7)	0.55(3)	0.84(2)	1.37(3)	0.35(7)	0.43(7)	0.57(4)	1.10(5)

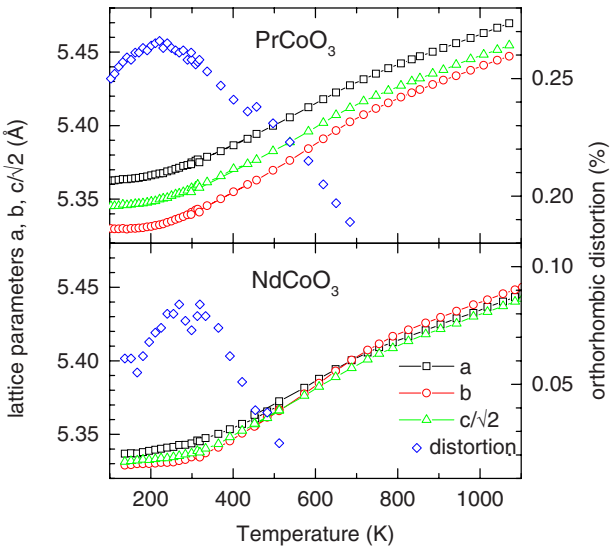

FIG. 2. (Color online) Temperature dependence of lattice parameters for $PrCoO_3$ and $NdCoO_3$.

$B=8\pi^2\langle u^2\rangle$. The values for Co atoms increase slightly linearly over the whole temperature range whereas in the case of Pr, Nd, and O atoms the increase at high temperature is more pronounced.

The averaged Co-O bond lengths for $PrCoO_3$ and $NdCoO_3$ are displayed in the upper panel of Fig. 4. For comparison, the data of $LaCoO_3$ (Ref. 3) and high-temperature data of $YCoO_3$ (Ref. 9) are also included, although the latter contain only a few temperature points and are less accurate. It is seen that the onset of Co-O expansion shifts systematically with diminishing Ln cation, and the bond lengths increase anomalously over the temperature range where the spin transitions take place. The bond lengths again merge together above 800 K.

The temperature dependence of averaged Co-O-Co bond angles is displayed in the lower panel of Fig. 4 also in comparison with $LaCoO_3$ and $YCoO_3$. The results show that the slope of the low-temperature bond-angle dependence is positive and approximately the same for all compounds up to 400 K. This behavior reflects a higher thermal expansion of ionic Ln-O bonds compared to more covalent Co-O bonds. There

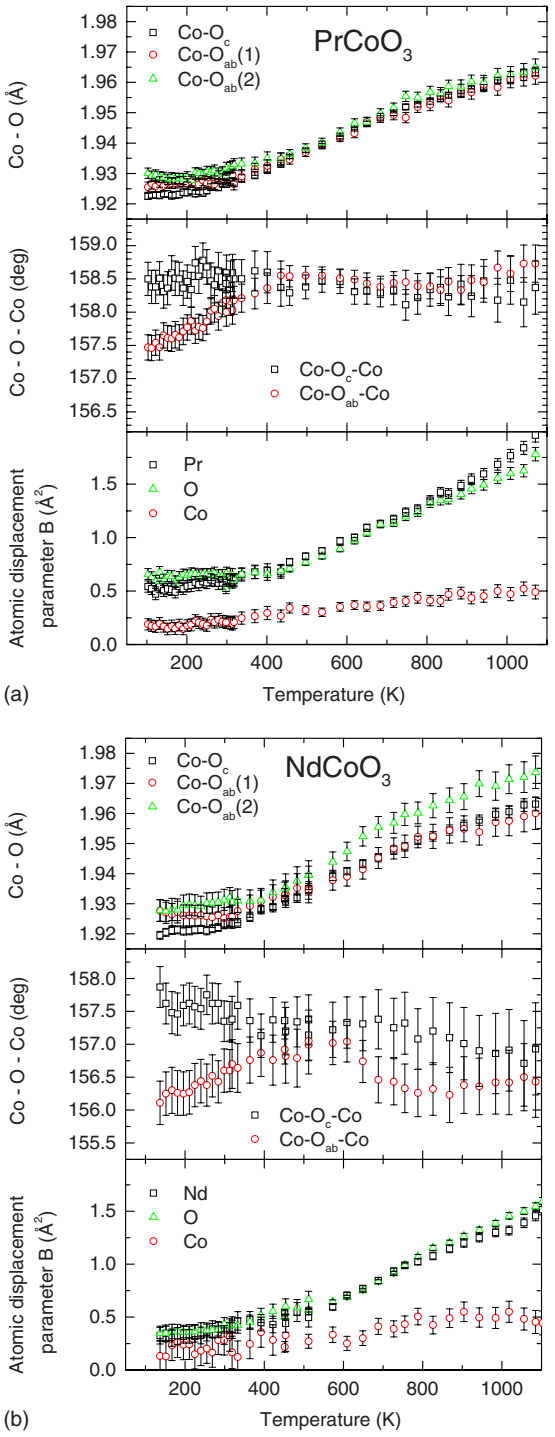

FIG. 3. (Color online) Observed bond lengths Co-O (upper), bond angles Co-O-Co (middle), and isotropic atomic displacement parameters B (lower) of $PrCoO_3$ and $NdCoO_3$.

is no observable anomaly in the Co-O-Co bond angles at the first spin transition (~70 K for $LaCoO_3$, ~260 K for $PrCoO_3$, and ~340 K for $NdCoO_3$). At elevated temperatures, only a weak anomaly is observed for $LaCoO_3$ with the onset of second spin transition at 500 K, whereas in the case of $PrCoO_3$ and $NdCoO_3$ there is a notable drop of the Co-O-Co angles in the vicinity of the critical temperatures of 600 and 630 K. Similar behavior may be detected also for

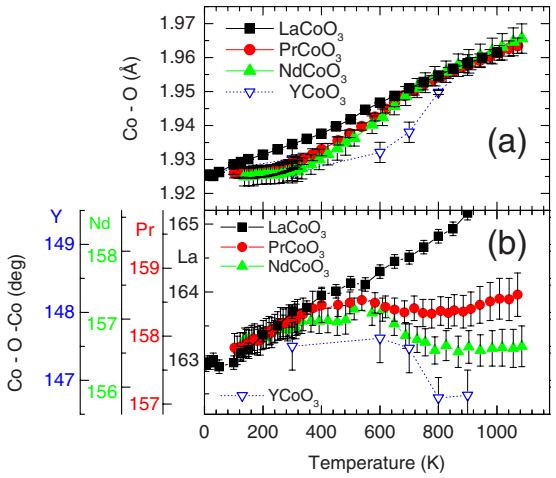

FIG. 4. (Color online) (a) Averaged bond lengths Co-O and (b) averaged bond angles Co-O-Co for $PrCoO_3$ and $NdCoO_3$ compared with $LaCoO_3$ (Ref. 3) and $YCoO_3$ (Ref. 9).

$YCoO_3$, but in that case the two spin transitions cannot be separated in temperature.

We speculate that the high-temperature decrease in Co-O-Co angles is a complex effect of different thermal dilatation of Ln-O bonds for different kinds of rare-earth cations and steric conditions in the ($Pbnm$) perovskite structure. It is also consistent with the LS-LS/HS-IS model of Co^{3+} spin transitions.[6,16,17] In the first spin transition, the excited HS sites are isolated and their expansion is partially compensated by shrinking and distortion of LS neighbors. When this transition in $LnCoO_3$ is shifted with decreasing Ln size to higher temperatures, the equilibrium number of excitations, obeying the standard Boltzmann statistics, develops with temperature more diffusively and the anomalous dilatation effect becomes less obvious. On the other hand, the second transition is associated with formation of a static IS phase of metallic character and is more localized in temperature. The excited IS states form clusters and the expansion of the CoO_6 octahedra in IS state must be compensated by their increased tilting. The decrease in Co-O-Co angles is more pronounced for $LnCoO_3$ with smaller rare-earth metal and higher degree of tilting. As concerns the absence of such effect for $LaCoO_3$ the reason might be in higher symmetry of $LaCoO_3$ structure ($R\bar{3}c$) and closeness of the transition to a cubic high-temperature structure.

The two transitions in $PrCoO_3$ and $NdCoO_3$ are further manifested in Fig. 5 as anomalous contribution to heat capacity measured at constant pressure (C_p). The base line is determined as a sum of lattice specific heat at constant volume, correction for normal dilatation and Schottky-type term due to crystal-field splitting of Pr^{3+} or Nd^{3+} electronic levels. It is seen that the excess heat exhibits maxima at respective transition temperatures.

In order to go into more detail, let us note that the heat capacity is basically composed of four significant contributions:

$$C_p = C_{V,\text{lattice}} + C_{\text{dilatation}} + C_{\text{magnetic}} + C_{\text{electronic}}, \qquad (1)$$

where the meaning of respective contributions is straightforward. The first and dominant term, $C_{V,\text{lattice}}$, is associated

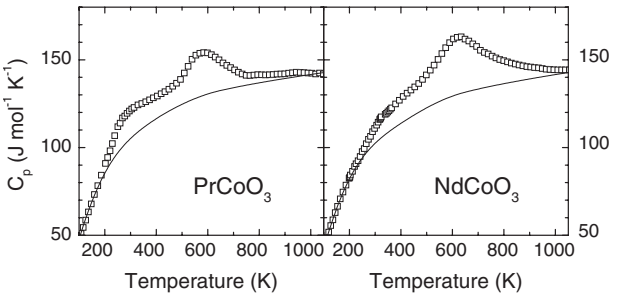

FIG. 5. Specific heat of $PrCoO_3$ and $NdCoO_3$. The calculated base lines [see Eq. (2)] are indicated by solid line.

with lattice dynamics which involves in the case of pseudocubic $LnCoO_3$ perovskites two acoustic-phonon bands (longitudinal and transversal) and eight optical-phonon bands. This fact makes the exact determination of phonon contribution over the whole temperature range rather difficult. Considering a relevant physical model with reasonable number of parameters, it is tentatively possible to combine the Debye term, reflecting the essential acoustic dynamics of the perovskite lattice, with several Einstein terms associated with CoO_6 octahedra and large cation optical vibrations (see, e.g., Refs. 18 and 19). Another possibility of how to determine the lattice contribution to the heat capacity is empirical—the application of measured data on structurally and chemically closely related compounds which do not exhibit crystallographic or electronic transitions; the suitable examples for our perovskites can be thus $LnGaO_3$ or $LnAlO_3$.[16] Nevertheless, for the sake of simplicity and considering the temperature range $T>150$ K, the lattice term can with a very good accuracy formally be modeled by a single Debye term, disregarding the weakness of its physical background. The obtained Debye temperatures are $\Theta_D=630$ K for $PrCoO_3$ and $\Theta_D=660$ K for $NdCoO_3$. At high temperatures well above Θ_D the heat capacity at constant volume C_V extrapolates to the well-known Dulong-Petit high-temperature limit which represents for the considered perovskites with five atoms in the primitive cell the high-temperature saturation at $15R \simeq 125$ J K^{-1} mol^{-1}.

The second contribution $C_{\text{dilatation}}$ reflects both the harmonic and anharmonic effects associated with lattice dilatation. In the simplest way the difference between the heat capacity at constant pressure and constant volume is expressed as $C_p - C_V = TV\alpha^2\beta^{-1}$, where T is thermodynamic temperature, V is a molar volume ($\approx 34\times10^{-6}$ m^3 for $LnCoO_3$ perovskites), β is isothermal compressibility ($\approx 7\times10^{-12}$ Pa^{-1}), and α is a coefficient of volume thermal expansion (saturated at $\approx 60\times10^{-6}$ K^{-1} above Θ_D).

The third and fourth contributions are due to additional degrees of freedom associated with electrons in incompletely filled shells or bands. They can contribute both to C_{magnetic}, via spin and orbital moments formed by localized electrons, and $C_{\text{electronic}}$ due to thermal excitations of bandlike electrons at Fermi level. The C_{magnetic} contribution in the case of $LnCoO_3$ perovskites comes not only from the spin transitions of cobalt subsystem ($C_{\text{Co,spin}}$) but also from the crystal-field splitting of the rare-earth electronic ground state ($C_{\text{Ln,CF}}$). In particular, there are nine singlets of $^3H_4$ parentage for Pr^{3+},

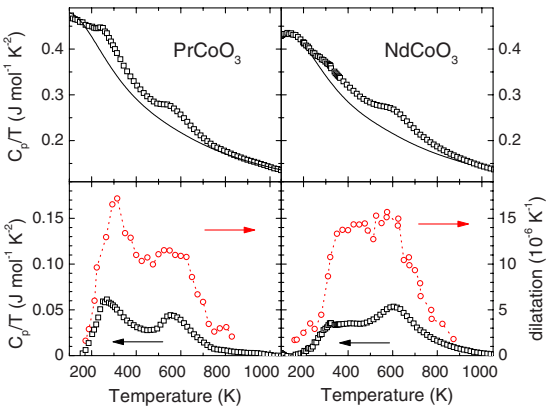

FIG. 6. (Color online) Upper panels: specific heat divided by temperature of $PrCoO_3$ and $NdCoO_3$. The calculated base lines [see Eq. (2)] are indicated by solid line. Lower panels: excess of specific heat divided by temperature compared with anomalous lattice thermal dilatation.

spread over 110 meV range[20] and five Kramers doublets of $^4I_{9/2}$ parentage for Nd^{3+}, spread over 70 meV range.[21] The excitations within these multiplets give rise to a Schottky-type contribution to the specific heat with a maximum of ≈ 5 J K^{-1} mol^{-1} around 90 K and approximately linear decrease above this temperature down to ≈ 1 J K^{-1} mol^{-1} at 1000 K.

Using the above-introduced notations, the base line in Figs. 5 and 6 is a sum of the following contributions:

$$C_{\text{base line}} = C_{V,\text{lattice}} + C_{\text{dilatation}} + C_{\text{Ln,CF}} \qquad (2)$$

The observed excess is thus related to the two remaining terms, $C_{\text{Co,spin}}$ and $C_{\text{electronic}}$. The former term is associated with the local transitions of cobalt ions while the latter one, anticipating an existence of bandlike charge carriers, contributes at high temperatures only where $LnCoO_3$ systems transform to a "metallic" state (see below). Generally, the electronic specific heat is represented as $C_E=\gamma T$. Nonetheless let us note that a simple extrapolation to high temperatures using the γ value determined (for samples with metallic ground state) at low temperatures is unphysical as the low temperature γ represents the highest limit significantly enhanced by electron correlations, electron-phonon interaction, or by a presence of sharp peak in density of states at E_F.

The excess specific heat associated with the Co-induced spin state or metal-insulator transitions is further depicted as a plot of C_p/T in Fig. 6. The data are compared with anomalous lattice dilatation calculated within a model adopted in our previous work[5] by subtracting the normal lattice dilatation from the observed dilatation (see Fig. 8 in Ref. 5 for details). It appears that the temperature course of C_{excess}/T, i.e., the accumulation of the entropy during the Co spin transitions, follows the temperature course of the dilatation anomaly (see the lower panels of Fig. 6). This is not surprising result since the simple thermodynamic (two-level) model of Co^{3+} excitations including also elastic energy of the solid shows that both the equilibrium volume $\Delta V=V-V_{\text{LS}}$ and the average thermal energy are proportional to the number of excited species. Another condition for the scaling is the ex-

perimental fact that both the integral volume change (about 1% for each transition; see Ref. 5) and the entropy change are distributed evenly between the two spin transitions.

The total change in entropy, after the spin-state transitions are accomplished, is determined to be ≈ 20 J K^{-1} mol^{-1} for both $PrCoO_3$ and $NdCoO_3$. These results can be compared with total entropy change determined previously from the heat capacity experiments for $LaCoO_3$ (26 J K^{-1} mol^{-1}) and $LnCoO_3$ with Ln=Sm–Lu (20–21 J K^{-1} mol^{-1}).[22] It should be noted that the larger value reported for $LaCoO_3$ might be overestimated due to uncertainty with subtraction of the lattice vibration term at low temperatures, which makes also difficult to estimate how entropy change is distributed. In the case of Sm–Lu, the two transitions coincide.

The observed entropy change between the LS ground state and the mixed phase with strong HS/LS correlations can be understood considering a pair model (see Ref. 6) with cobalt positions in alternative eigenstates (close to HS or to LS, with some admixtures). At the saturation (supposing that HS:LS ratio is close to 1:1), the entropy including both spin and orbital degeneracy would be $(1/2)R \ln 15 = 11.3$ J K^{-1} mol^{-1}. This is in agreement with present results for both $PrCoO_3$ and $NdCoO_3$. After the second transition is over, the system tends to a homogeneous metallic phase of IS character. As pointed out by Tachibana *et al.*,[22] the total excess of entropy is close to the theoretical value $R \ln 9 = 18.3$ J K^{-1} mol^{-1} expected for the localized Co^{3+} IS state. However, we assume as a more appropriate the "itinerant" picture of the Co^{3+} intermediate-spin state described as $t_{2g}^5 \sigma^{*1}$ with "degenerate" e_g electrons. Indeed the low resistivity (~ 2 mΩ cm) and low positive metallic thermopower at high temperature[5,23] support this picture. Thus the total excess entropy can be estimated as a sum of two components: (i) the first one being associated with the spin and orbital degeneracy of localized t_{2g} core and corresponding to the transition between the t_{2g}^6 and t_{2g}^5, which leads to $R \ln 6 = 14.9$ J K^{-1} mol^{-1} and (ii) the second one being associated with onset at the insulator-metal transition of bandlike carriers of e_g character. To estimate the entropy associated with this insulator-transition transition is difficult since all the $LnCoO_3$ phases possess an insulating ground state based on the LS Co^{3+}. Tentatively one may asses the bare γ on a base of *ab initio* calculations for IS phase. Preliminary results indicate for similar $LaCoO_3$ the $\gamma \sim 2-3$ mJ K^{-2} mol^{-1}. The experimentally determined entropy accumulated by the metallic e_g electrons after the insulator-metal transition is $\Delta S \approx 5$ J K^{-1} mol^{-1}, which in a first approximation provides a higher but still reasonable estimate of the linear coefficient of electronic specific heat $\gamma = 5-6$ mJ K^{-2} mol^{-1}.

IV. CONCLUSIONS

The perovskites $PrCoO_3$ and $NdCoO_3$ undergo two successive transitions associated with a change in spin state of Co^{3+} ions. The transitions give rise to anomalous contributions in the heat capacity and are manifested by pronounced changes in the thermal dilatation of the lattice parameters and Co-O bond distances. As regard to the Co-O-Co bond angles, there is no observable anomaly at the first spin transition, whereas the second transition is manifested by a notable drop in their temperature dependence. The experimental results are interpreted within with the LS-LS/HS-IS model in which the first step of this model involves excitation of diamagnetic LS Co^{3+} states to paramagnetic HS states and tends to a saturation with the HS/LS ratio close to 1:1. The observed entropy change is on the order of $\Delta S \approx 10$ J K^{-1} mol^{-1}, in agreement with $(1/2)R \ln 15 = 11.3$ J K^{-1} mol^{-1} expected for the spin and orbital degeneracy of the HS Co^{3+} ions. The second transition is associated with formation of a homogeneous IS phase of metallic character. It is accompanied with a similar increase in entropy, so that the total entropy change after the two transitions is ≈ 20 J K^{-1} mol^{-1}. This value can be understood considering that the main contribution comes from localized t_{2g}^5 electrons (formally the configuration entropy of LS Co^{4+} ions) amounting to $R \ln 6 = 14.9$ J K^{-1} mol^{-1} while the rest ≈ 5 J K^{-1} mol^{-1} is ascribed to the entropy accumulated by the bandlike e_g electrons which are formed at the insulator-metal transition (analogous to common electronic heat in metals).

ACKNOWLEDGMENTS

This work was supported by Project No. 202/09/0421 of the Grant Agency of the Czech Republic. We acknowledge the Institut Laue Langevin (Grenoble, France) and the Laboratoire Leon Brillouin (Saclay, France) for providing access to the neutron beams and for all technical support during the experiments.

[1] G. Demazeau, M. Pouchard, and P. Hagenmuller, J. Solid State Chem. **9**, 202 (1974).
[2] X. Liu and C. T. Prewitt, J. Phys. Chem. Solids **52**, 441 (1991).
[3] P. G. Radaelli and S.-W. Cheong, Phys. Rev. B **66**, 094408 (2002).
[4] C. Zobel, M. Kriener, D. Bruns, J. Baier, M. Grüninger, T. Lorenz, P. Reutler, and A. Revcolevschi, Phys. Rev. B **66**, 020402(R) (2002).
[5] K. Knížek, Z. Jirák, J. Hejtmánek, M. Veverka, M. Maryško, G. Maris, and T. T. M. Palstra, Eur. Phys. J. B **47**, 213 (2005).
[6] K. Knížek, Z. Jirák, J. Hejtmánek, P. Henry, and G. André, J. Appl. Phys. **103**, 07B703 (2008).
[7] K. Berggold, M. Kriener, P. Becker, M. Benomar, M. Reuther, C. Zobel, and T. Lorenz, Phys. Rev. B **78**, 134402 (2008).
[8] A. Mehta, R. Berliner, and R. W. Smith, J. Solid State Chem. **130**, 192 (1997).
[9] K. Knížek, Z. Jirák, J. Hejtmánek, M. Veverka, M. Maryško, B. C. Hauback, and H. Fjellvåg, Phys. Rev. B **73**, 214443 (2006).
[10] A. P. Sazonov, I. O. Troyanchuk, V. Sikolenko, G. M. Chobot,

and H. Szymczak, J. Phys.: Condens. Matter **17**, 4181 (2005).
[11] C. Tealdi, L. Malavasi, F. Gozzo, C. Ritter, M. C. Mozzati, G. Chiodelli, and G. Flor, Chem. Mater. **19**, 4741 (2007).
[12] H. W. Brinks, H. Fjellvåg, A. Kjekshus, and B. C. Hauback, J. Solid State Chem. **147**, 464 (1999).
[13] J. A. Alonso, M. J. Martínez-Lope, C. de la Callea, and V. Pomjakushin, J. Mater. Chem. **16**, 1555 (2006).
[14] M. Marezio, J. P. Remeika, and P. D. Dernier, Acta Crystallogr., Sect. B: Struct. Crystallogr. Cryst. Chem. **26**, 2008 (1970).
[15] W. Sławiński, R. Przeniosło, I. Sosnowska, and E. Suard, J. Phys.: Condens. Matter **17**, 4605 (2005).
[16] T. Kyômen, Y. Asaka, and M. Itoh, Phys. Rev. B **71**, 024418 (2005).
[17] K. Knížek, Z. Jirák, J. Hejtmánek, P. Novák, and Wei Ku, Phys. Rev. B **79**, 014430 (2009).
[18] J. T. Last, Phys. Rev. **105**, 1740 (1957).
[19] D. Sedmidubský, A. Strejc, O. Beneš, K. Ružička, J. Hejtmánek, P. Javorský, M. Nevřiva, and C. Martin, J. Solid State Chem. **179**, 3798 (2006).
[20] A. Podlesnyak, S. Rosenkranz, F. Fauth, W. Marti, H. J. Scheel, and A. Furrer, J. Phys.: Condens. Matter **6**, 4099 (1994).
[21] A. Podlesnyak, S. Rosenkranz, F. Fauth, W. Marti, A. Furrer, A. Mirmelstein, and H. J. Scheel, J. Phys.: Condens. Matter **5**, 8973 (1993).
[22] M. Tachibana, T. Yoshida, H. Kawaji, T. Atake, and E. Takayama-Muromachi, Phys. Rev. B **77**, 094402 (2008).
[23] S. Yamaguchi, Y. Okimoto, and Y. Tokura, Phys. Rev. B **54**, R11022 (1996).